Generalized Scattering Matrix Method for Analysis of Cascaded and Offset Microstrip Step Discontinuities

TAK SUM CHU AND TATSUO ITOH, FELLOW, IEEE

Abstract—**Detailed algorithms are presented for characterizations of cascaded microstrip step discontinuities, symmetric stubs, and offset step. The analysis is based on the generalized scattering matrix techniques after the equivalent waveguide model is introduced for the microstrip line.**

I. Introduction

THE EQUIVALENT waveguide model has been advantageously used for characterizing a number of discontinuities appearing in microstrip circuits [1]–[3]. Although the radiation and surface-wave excitation are neglected, these characterizations provide useful and accurate information in many practical applications. Formulations for these discontinuity problems are typically done by the mode-matching technique. However, detailed formulation algorithms are not readily available.

Recently, the present authors carried out an assessment for a number of different formulations for a microstrip step discontinuity within the framework of the waveguide model. The most economical and yet most accurate formulation was suggested [4]. The step discontinuity has also been analyzed by the modified residue calculus technique (MRCT) [5].

The present paper extends the analysis of the step discontinuity to a cascaded step discontinuity and an offset step discontinuity. The symmetric stub can be treated as the cascaded step discontinuity. The offset discontinuity will be treated as the limiting case of a cascaded discontinuity. In each case, the individual step discontinuity is characterized by either the MRCT or the mode-matching method. The analysis results in a generalized scattering matrix for each step. The analysis of the cascaded step is undertaken by invoking the generalized scattering matrix technique in which the generalized scattering matrices of two step junctions are combined [6], [7]. The ultimate result is the generalized scattering matrix of the cascaded junction as a whole.

It should be noted that the waveguide model is presumed to be an acceptable model for the present analysis. The results are compared with the experimental data as well as those reported in the literature.

Manuscript received August 2, 1985; revised October 1, 1985. This work was supported in part by the U.S. Army Research Office, under Contract DAAG29-84-K-0076.

The authors are with the Electrical Engineering Research Laboratory, University of Texas, Austin, TX 78712.

IEEE Log Number 8406468.

II. Formulation of the Problem

A. Cascaded Step Discontinuity

The algorithm for the analysis will be best illustrated by means of the cascaded step discontinuity. Specific changes required for the offset discontinuity will be explained later. The first step of the analysis is to replace the microstrip circuit under study with its equivalent waveguide model [8]. The top and bottom are electric walls and the sidewalls are magnetic walls. The height h in Fig. 1 remains unchanged. The effective dielectric constant ϵ_1 and the effective width $\overline{W}_1$ of region I with the microstrip width W_1 can be found from the dominant mode phase constant β_1 and the characteristic impedance Z_{01} of the microstrip line

$$\epsilon_1 = (\beta_1/k_0)^2 \tag{1}$$

$$Z_{01} = \left[120\pi/\sqrt{\epsilon_1}\right](h/\overline{W}_1). \tag{2}$$

β_1 and Z_{01} must be calculated from the structural parameters by a standard full-wave analysis [9], [10] or a curve-fit formula [11]. Other regions may be modeled in a similar manner.

The next step is to characterize all the discontinuities involved in the waveguide model of the microstrip circuit under study. This characterization is done in terms of the generalized scattering matrix [6], [7]. This matrix is closely related to the scattering matrix used in the microwave network theory, but differes in that the dominant as well as higher order modes are included. Therefore, the generalized scattering matrix will be, in general, of infinite order. Consider, for instance, the TE_{p0} excitation with unit amplitude from the left to junction 1 in Fig. 2. If the amplitude of the nth mode of the reflected wave to the left is A_n, the (n, p) entry of the scattering matrix $S^{11}(n, p)$ is A_n. Similarly, if the amplitude of the mth mode of the wave transmitted to the right in B_m, $S^{21}(m, p)$ is B_m. Other matrix elements can be derived similarly. Hence, the generalized scattering matrix S_1 of the junction 1 can be written in terms of four submatrices of infinite order

$$S_1 = \begin{bmatrix} S^{11} & S^{12} \\ S^{21} & S^{22} \end{bmatrix}. \tag{3}$$

The corresponding matrix of the junction 2 is

$$S_2 = \begin{bmatrix} S^{33} & S^{34} \\ S^{43} & S^{44} \end{bmatrix}. \tag{4}$$

0018-9480/86/0200-0280$01.00 ©1986 IEEE

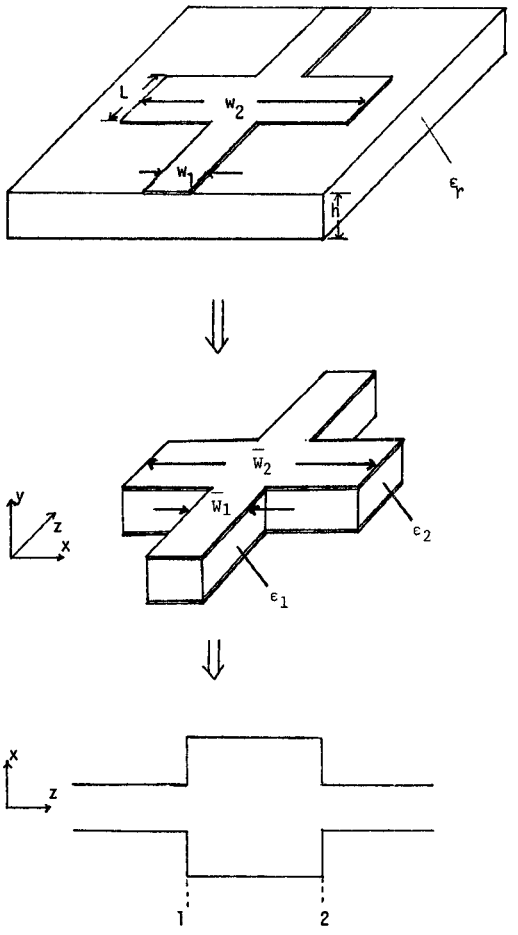

Fig. 1. Cascaded step discontinuities, equivalent waveguide model, and top view.

All of the elements of the generalized scattering matrix can be obtained by solving the electromagnetic problem of the junction scattering by means of a standard technique such as the mode-matching technique [4] or a modified residue calculus technique [5]. Since the details of these methods for an isolated step discontinuity are reported in [4] and [5], they are not repeated here. We presume all of these quantities are now available.

The remaining step is to combine these generalized scattering matrices of the cascaded junctions and to derive the composite matrix.

$$S = \begin{bmatrix} S^{AA} & S^{AC} \\ S^{CA} & S^{CC} \end{bmatrix}. \tag{5}$$

To this end, we introduce the transmission matrix $S^{(L)}$ of the waveguide between junctions 1 and 2. The wave travels a distance L so that each mode is multiplied by $\exp(-\gamma L)$

$$S^{(L)} = \begin{bmatrix} e^{-\gamma_1 L} & & & 0 \\ & e^{-\gamma_2 L} & & \\ & & \ddots & \\ 0 & & & e^{-\gamma_n L} \end{bmatrix} \tag{6}$$

where γ_n is the propagation constant of the nth mode of Region B. Hence $\gamma_1 = j\beta_2 L$, where β_2 is the dominant-mode phase constant of Region B. Our algebraic process to

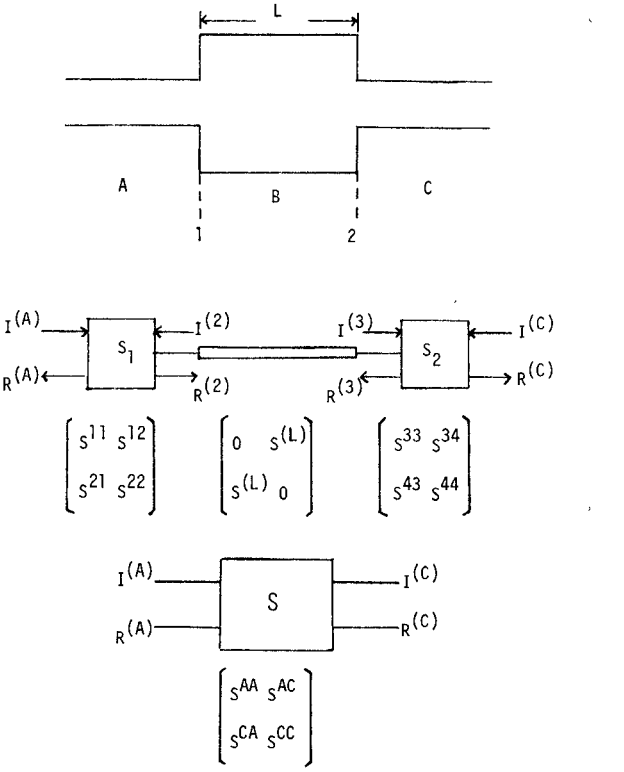

Fig. 2. Derivation of S parameters for the cascaded step discontinuity structures.

derive S is detailed in the Appendix. The results are

$$S^{AA} = S^{11} + S^{12}S^{(L)}U_2S^{33}S^{(L)}S^{21} \tag{7a}$$

$$S^{AC} = S^{12}S^{(L)}U_2S^{34} \tag{7b}$$

$$S^{CA} = S^{43}S^{(L)}U_1S^{21} \tag{7c}$$

$$S^{CC} = S^{44} + S^{43}S^{(L)}U_1S^{22}S^{(L)}S^{34} \tag{7d}$$

where

$$U_1 = (I - S^{22}S^{(L)}S^{33}S^{(L)})^{-1} \tag{8a}$$

$$U_2 = (I - S^{33}S^{(L)}S^{22}S^{(L)})^{-1} \tag{8b}$$

and I is the unit matrix. The above matrices are formally of infinite size. However, in practice, these matrices must be truncated to a finite size. It is found that excellent convergence is obtained when 3×3 or even 2×2 submatrices S^{11}, etc., are used.

It should be noted here that the use of generalized scattering matrices is increasingly more important as the distance between two junctions is smaller. Therefore, the present technique can be used for analysis of the symmetric stub from the knowledge of the generalized scattering matrix of a single step discontinuity.

B. Offset Step Discontinuity

Next, the technique described above will be applied to an offset step discontinuity shown in Fig. 3. This offset discontinuity occurs in a microstrip circuit either intentionally or unintentionally. As we will see shortly, a small amount of offset Δ significantly affects the scattering characteristic of the discontinuity.

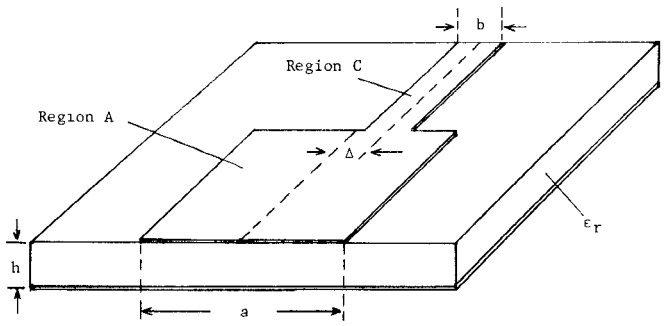

Fig. 3. Offset step discontinuity with eccentricity Δ.

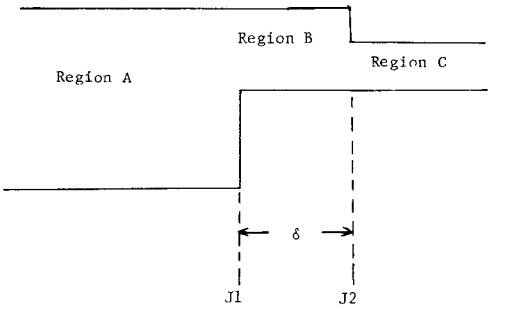

Fig. 5. Auxiliary structure of the offset step for the generalized scattering matrix technique.

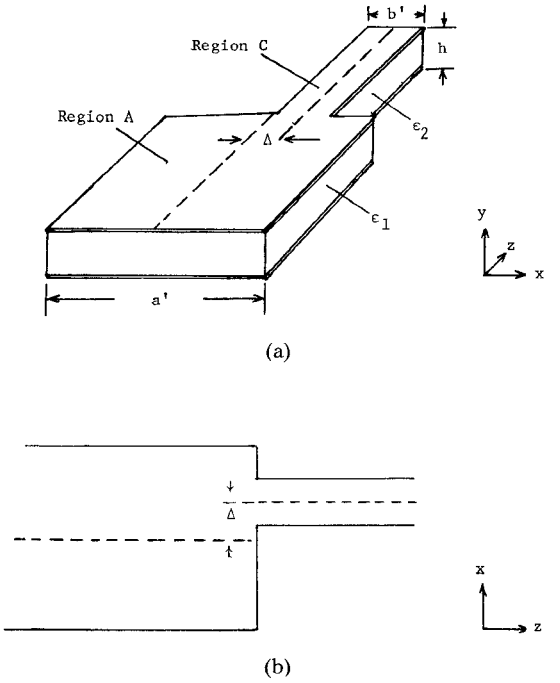

Fig. 4. Equivalent waveguide model of the offset step: (a) perspective view and (b) top view.

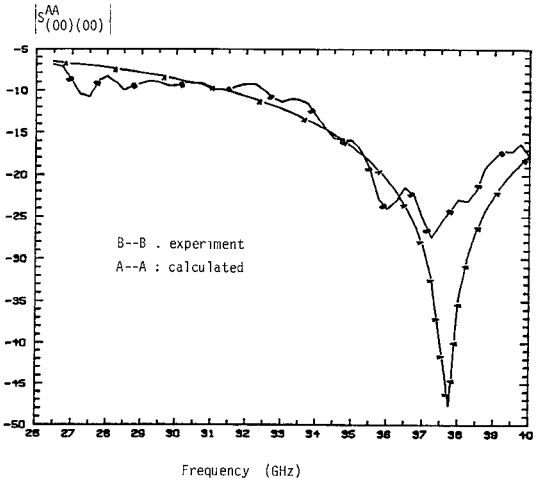

Fig. 6. Numerical data for the cascaded step.

Once again, the first step is to derive the equivalent waveguide model depicted in Fig. 4. Although a direct formulation of Fig. 4 is possible by way of the mode-matching technique, we will take an alternative approach in which the formulations and the generalized scattering matrices of the symmetric step discontinuities are advantageously used. To this end, an auxiliary structure in Fig. 5 is introduced. Notice that the original offset step discontinuity structure can be recovered by letting δ in Fig. 5 to zero after all the formulations are carried out. Also, the individual discontinuities $J1$ and $J2$ in Fig. 5 are one-half of the symmetric step discontinuities. Hence, all of the previous results for the symmetric step discontinuities excited by the even-mode can be directly used. In fact, in [4] and [5], only one-half of the structure has been used for analysis.

Once the scattering matrices of $J1$ and $J2$ are available, the scattering matrix of the composite discontinuity can be derived from (7) and (8) except that $S^{(L)} = I$ when $\delta \to 0$. This completes the formulation for the offset discontinuity.

III. Results and Discussions

Fig. 6 shows typical results of the amplitude of the dominant mode (quasi-TEM) reflection coefficient from a cascaded step discontinuity. The results are found to agree very well with the experimental data taken at Hughes Torrance Research Center for the microstrip circuit on a Duroid substrate.

For efficient calculation, it is desirable to be able to truncate the matrices at as small a size as possible with accurate results. In the case of the cascaded discontinuity, $S^{(L)}$ contains a convergent factor since all of the higher order modes have real values of γ_n. In the case of an offset discontinuity, such exponentially decaying factors disappear because the length $\delta \to 0$, and hence $S^{(L)} = I$. To test the convergence of the solution, the dominant-mode transmission coefficient calculated using generalized scattering matrices of sizes 2×2, 3×3, and 5×5 are compared. Physical parameters are chosen to be the same as those studied by Kompa [12] so as to permit a comparison of results. Fig. 7 shows the results of this convergence study. It is seen that even the 2×2 matrix gives reasonably accurate results. To establish the validity of the results, they are compared with those calculated by Kompa [12]. This comparison is shown in Fig. 8(a) and (b). Finally, the dominant-mode transmission coefficient for various eccentricities are calculated. It is evident in Fig. 9 that the

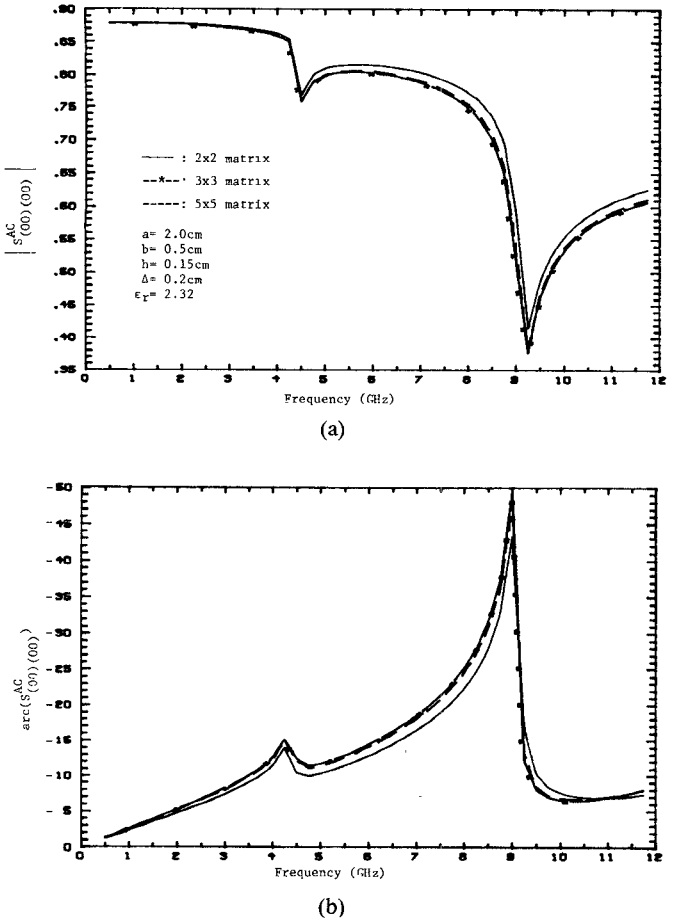

Fig. 7. Convergence study of the generalized scattering matrix technique for an offset step: (a) magnitude and (b) phase.

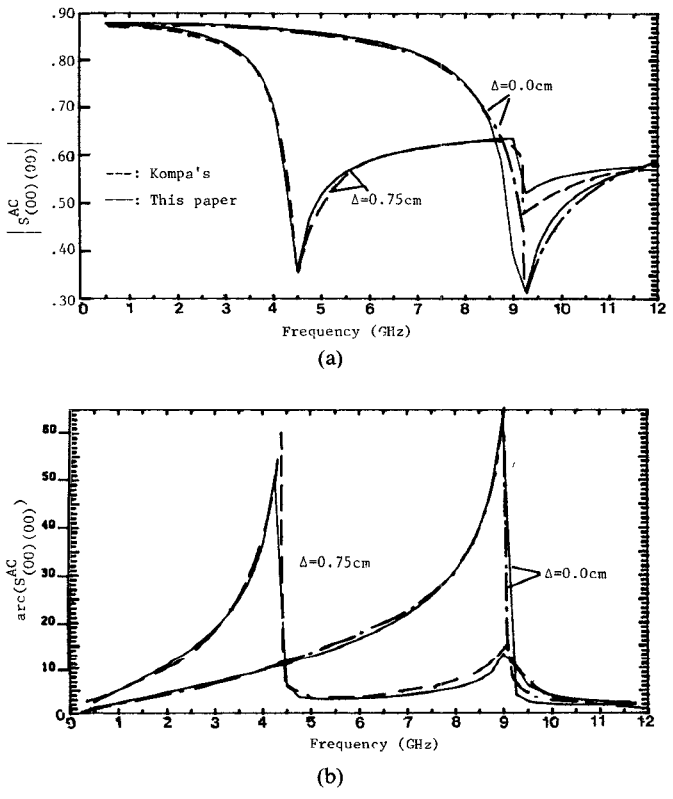

Fig. 8. Comparison with Kompa's results: (a) magnitude and (b) phase.

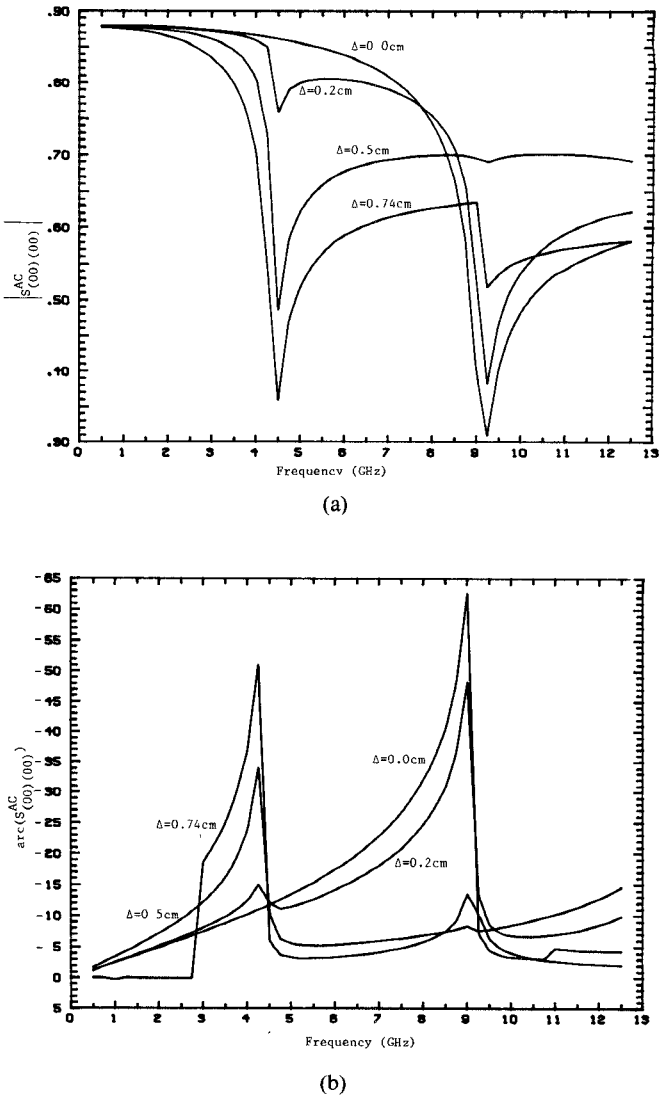

Fig. 9. Effect of eccentricity: (a) magnitude and (b) phase.

effect of the first odd-mode cutoff is exhibited as soon as the eccentricity is nonzero. Also, for $\Delta = 0.5$ cm, the effect of the second- (even-) mode cutoff is quite small due to the fact that the center of the smaller waveguide is located at the second-mode null and, hence, little coupling via this mode exists.

IV. Conclusions

The generalized scattering matrix technique has been applied to the problems of a cascaded step discontinuity and an offset step discontinuity. The waveguide model has been presumed to be applicable for analysis. Individual discontinuities are characterized first and the results are used for the description of the composite discontinuity via the generalized scattering matrix technique. In spite of the two-step process, the overall effort in numerical processing is quite efficient. In actual numerical software, the programs for isolated discontinuities can be used as subroutines for the composite structures.

APPENDIX
DERIVATION OF SCATTERING MATRIX FOR THE CASCADED STEP DISCONTINUITIES

The following matrix equations can be derived from Fig. 2:

$$\begin{bmatrix} R^{(A)} \\ R^{(2)} \end{bmatrix} = \begin{bmatrix} S^{11} & S^{12} \\ S^{21} & S^{22} \end{bmatrix} \begin{bmatrix} I^{(A)} \\ I^{(2)} \end{bmatrix} \tag{A1}$$

$$\begin{bmatrix} I^{(2)} \\ I^{(3)} \end{bmatrix} = \begin{bmatrix} 0 & S^{(L)} \\ S^{(L)} & 0 \end{bmatrix} \begin{bmatrix} R^{(2)} \\ R^{(3)} \end{bmatrix} \tag{A2}$$

$$\begin{bmatrix} R^{(3)} \\ R^{(C)} \end{bmatrix} = \begin{bmatrix} S^{33} & S^{34} \\ S^{43} & S^{44} \end{bmatrix} \begin{bmatrix} I^{(3)} \\ I^{(C)} \end{bmatrix}. \tag{A3}$$

Next, (A2) is substituted into (A1) to get

$$R^{(A)} = S^{11}I^{(A)} + S^{12}S^{(L)}R^{(3)} \tag{A4}$$

$$R^{(2)} = S^{21}I^{(A)} + S^{22}S^{(L)}R^{(3)}. \tag{A5}$$

Next, (A2) is substituted into (A3) to get

$$R^{(3)} = S^{33}S^{(L)}R^{(2)} + S^{34}I^{(C)} \tag{A6}$$

$$R^{(C)} = S^{43}S^{(L)}R^{(2)} + S^{44}I^{(C)}. \tag{A7}$$

Equations (A5) and (A6) are used to isolate $R^{(2)}$ and $R^{(3)}$

$$R^{(2)} = U_1 S^{21} I^{(A)} + U_1 S^{22} S^{(L)} S^{34} I^{(C)} \tag{A8}$$

where

$$U_1 = \left(I - S^{22}S^{(L)}S^{33}S^{(L)}\right)^{-1}$$

and

$$R^{(3)} = U_2 S^{33} S^{(L)} S^{21} I^{(A)} + U_2 S^{34} I^{(C)} \tag{A9}$$

where

$$U_2 = \left(I - S^{33}S^{(L)}S^{22}S^{(L)}\right)^{-1}.$$

Finally, (A8) and (A9) are substituted into (A4) and (A7) to get

$$\begin{aligned} R^{(A)} &= S^{11}I^{(A)} + S^{12}S^{(L)}U_2S^{33}S^{(L)}S^{21}I^{(A)} \\ &\quad + S^{12}S^{(L)}U_2S^{34}I^{(C)} \\ R^{(C)} &= S^{43}S^{(L)}U_1S^{21}I^{(A)} \\ &\quad + S^{43}S^{(L)}U_1S^{22}S^{(L)}S^{34}I^{(C)} + S^{44}I^{(C)}. \end{aligned}$$

S^{AA}, S^{AC}, S^{CA}, and S^{CC} can be identified easily from the above equations.

ACKNOWLEDGMENT

The authors thank Dr. Y. C. Shih of Hughes Torrance Research Center for providing experimental data and for technical discussions.

REFERENCES

[1] I. Wolff, G. Kompa, and R. Mehran, "Calculation method for microstrip discontinuities and T-junctions," *Electron. Lett.*, vol. 8, pp. 177–179, Apr. 1972.
[2] G. Kompa, "*S*-matrix computation of microstrip discontinuities with a planar waveguide model," *Arch. Elek. Übertragung.*, vol. 30, pp. 58–64, Feb. 1976.
[3] W. Menzel and I. Wolff, "A method for calculating the frequency-dependent properties of microstrip discontinuities," *IEEE Trans. Microwave Theory Tech.*, vol. MTT-25, pp. 107–112, Feb. 1977.
[4] T. S. Chu, T. Itoh, and Y-C. Shih, "Comparative study of mode-matching formulations for microstrip discontinuity problems," *IEEE Trans. Microwave Theory Tech.*, vol. MTT-33, pp. 1018–1023, Oct. 1985.
[5] T. S. Chu and T. Itoh, "Analysis of microstrip step discontinuity by the modified residue calculus technique," *IEEE Trans. Microwave Theory Tech.*, vol. MTT-33, pp. 1024–1028, Oct. 1985.
[6] J. Pace and R. Mittra, "Generalized scattering matrix analysis of waveguide discontinuity problems," in *Quasi-Optics XIV*. New York: Polytechnic Institute of Brooklyn Press, 1964, pp. 172–194.
[7] Y.-C. Shih, T. Itoh, and L. Q. Bui, "Computer-aided design of millimeter-wave *E*-plane filters," *IEEE Trans. Microwave Theory Tech.*, vol. MTT-31, pp. 135–142, Feb. 1983.
[8] I. Wolff and N. Knoppik, "Rectangular and circular microstrip disk capacitors and resonators," *IEEE Trans. Microwave Theory Tech.*, vol. MTT-22, pp. 857–864, Oct. 1974.
[9] T. Itoh, "Spectral domain immittance approach for dispersion characteristics of generalized printed transmission lines," *IEEE Trans. Microwave Theory Tech.*, vol. MTT-28, pp. 733–736, July 1980.
[10] R. Jansen and M. Kirschning, "Arguments and an accurate model for the power-current formulation of microstrip characteristic impedance," *Arch. Elek. Übertragung.*, vol. 37, pp. 108–112, Mar. 1983.
[11] E. Hammerstad and O. Jensen, "Accurate models for microstrip computer-aided design," in *IEEE MTT-S Int. Symp. Dig.* (Washington, DC), 1980, pp. 407–409.
[12] G. Kompa, "Frequency-dependent behavior of microstrip offset junction," *Electron. Lett.*, vol. 11, no. 22, pp. 172–194, Oct. 1975.

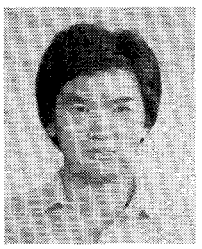

Tak Sum Chu was born in Kowloon, Hong Kong, on October 4, 1960. He received the B.S. degree in electrical engineering from the University of Texas at Austin in 1982. Currently, he is working towards the M.S. degree at the University of Texas.

Tatsuo Itoh (S'69–M'69–SM'74–F'82) received the Ph.D. degree in electrical engineering from the University of Illinois, Urbana, in 1969.

From September 1966 to April 1976, he was with the Electrical Engineering Department, University of Illinois. From April 1976 to August 1077, he was a Senior Research Engineer in the Radio Physics Laboratory, SRI International, Menlo Park, CA. From August 1977 to June 1978, he was an Associate Professor at the University of Kentucky, Lexington. In July 1978, he joined the faculty of the University of Texas at Austin, where he is now a Professor of Electrical Engineering and Director of the Microwave Laboratory. During the summer of 1979, he was a Guest Researcher at AEG-Telefunken, Ulm, West Germany. Since 1983, he has held the Hayden Head Professorship in Engineering.

Dr. Itoh is a member of the Institute of Electronics and Communication Engineers of Japan, Sigma Xi, and Commissions B and C of USNC/URSI. He is a Professional Engineer registered in the State of Texas.